DOI: 10.1007/s12541-012-0233-x

Design of Joint Torque Sensor with Reduced Torque Ripple for a Robot Manipulator

In-Moon Kim[1], Hwi-Su Kim[1], and Jae-Bok Song[1,#]

1 School of Mechanical Engineering, Korea University, 5-1, Anam-dong, Seongbuk-gu, Seoul, Korea, 136-713
Corresponding Author / E-mail: jbsong@korea.ac.kr, TEL: +82-2-3290-3363, FAX: +82-2-3290-3757

KEYWORDS: Joint torque sensor, Service robot manipulator, Torque ripple, Harmonic drive

Joint torque sensors are widely used in service robots for force control and collision detection. However, commercial torque sensors and amplifiers are too bulky to install inside robots. In this study, we propose an amplifier-embedded torque sensor because placing the amplifier away from the sensor tends to add noise to the output signal. Furthermore, joint torque sensors experience the torque ripple generated by the harmonic drive gear. Therefore, a torque ripple reduction method is also proposed in this study. FEM analysis was conducted to improve the sensitivity of the torque sensor to only torques in the direction of joint rotation. To avoid external noise and excessive wiring, an embedded amplifier, which can be installed inside the joint of the robot arm with the torque sensor, was developed. Also, the torque ripple reduction method based on the change in the installation position of Wheatstone bridges was developed. Through various experiments, the performance of the proposed torque sensor was verified.

Manuscript received: January 12, 2012 / Accepted: May 14, 2012

1. Introduction

In general, a robot manipulator performs force control using a 6-axis forces/torque (F/T) sensor installed at its end-effector.[1] However, the use of these expensive F/T sensors tends to significantly increase the price of robots. Furthermore, this F/T sensor mounted at the wrist of a robot arm can detect only contacts at the end-effector since it cannot measure external forces applied to links other than the end-effector. However, if joint torque sensors are installed at each joint of a manipulator to directly measure torques,[2,3] manipulators can detect collision occurring not only at the end-effector but also at each link. Moreover, the external force applied to the end-effector can be estimated without the use of an expensive 6-axis F/T sensor.[4]

However, there have been several problems in the installation of joint torque sensors at each joint of a service robot arm. Most commercial torque sensors are not suitable for service robot arms due to their excessive size and weight. Also, a torque sensor requires an amplifier, but commercial amplifiers are too large to embed inside the link of a robot. Thus, the amplifiers are placed away from the robot with long wiring, which may induce undesirable noise in the output signal. To overcome these problems, a joint torque sensor should be small enough to fit into a robot arm and its amplifier should be embeddable into the sensor as well.

Furthermore, a torque sensor is often subject to torque ripple when it is used with a harmonic drive which is often employed in service robots due to its compact size, light weight and high gear reduction. However, a harmonic drive tends to induce a unique mechanical noise, which is also known as *torque ripple*. This torque ripple is characterized by periodic oscillation whose frequency varies depending on the angular velocity of the harmonic drive and whose magnitude is several times higher than that of ordinary electrical noise. Because of this varying frequency, it is difficult to apply a normal software filter (e.g., low-pass filter or band-pass filter) to remove this ripple. Therefore, such torque ripple significantly deteriorates the performances of force control and collision detection of a manipulator. To deal with these problems, a torque ripple reduction method should be applied to the joint torque sensor. Several methods were proposed to reduce torque ripple: modeling the mechanical properties of the harmonic drive,[5,6] applying a Kalman filter,[7] attaching strain gauges on the flexspline of the harmonic drive,[7-9] and applying a switching notch filter.[10]

However, these previous approaches were not effective in successfully eliminating torque ripple. A harmonic drive is difficult to model because of its complex structure. The parameters have to be identified regularly since the characteristics of a harmonic drive change with the lubrication condition. A Kalman filter, on the other hand, may induce a time delay, and requires an appropriate error

model. Placing strain gauges on the flexspline can be a useful solution, but strain gauges must be placed at exact positions and in exact orientations. The switching notch filter also induces a time delay, which is not desirable.

In this paper, we propose a joint torque sensor for a service robot arm. The joint torque sensor is compact and lightweight and includes an embedded amplifier that enables a digital torque signal output. Moreover, we propose a novel torque ripple reduction method that uses two Wheatstone bridge circuits to effectively eliminate torque ripple. The proposed reduction method does not induce any time delay unlike software filtering which requires computational burden.

This paper is organized as follows. Section 2 presents the structure of the proposed joint torque sensor, Wheatstone bridge and amplifier. Section 3 describes the cause of torque ripple and the reduction method. The sensing performance of the proposed joint torque sensor and the effectiveness of the proposed torque ripple reduction method are evaluated in Section 4. Finally, Section 5 presents our conclusions.

2. Joint Torque Sensor

In this study, we designed a compact joint torque sensor to install at each joint of a manipulator to measure external torques. It was designed to be sensitive to the torque in the direction of joint rotation, but insensitive to the other directions to measure only joint torques at each joint. Furthermore, we developed an amplifier that could be embedded into the sensor module. In this section, the structure and circuit design of the proposed joint torque sensor will be presented.

2.1 Structure Design

A joint torque sensor should deform linearly in response to an external torque. Strain gauges are usually used to measure the deformation $\delta\theta$ due to an applied external torque. The measured deformation is then converted to the torque τ according to the following equation.

$$\tau = k_t \cdot \delta\theta \tag{1}$$

where k_t is the rotational stiffness of the sensing element. As shown in Fig. 1, the joint torque sensor is usually installed between the speed reducer and the output link.

The maximum size, capacity and safety factor of a typical service robot arm were considered in designing the joint torque sensor. The joint torque sensor shown in Fig. 2 has a unique hub-spoke shape with slits, which makes the sensor more sensitive to an external torque.[11] The joint torque sensor is made of aluminum alloy for light weight, and has a hollow hole for wiring.

To find the optimal locations for strain gauge attachment (i.e., locations of maximum strain), FEM analysis of the structure shown in Fig. 2(a) was performed. In general, the maximum strain of an aluminum alloy structure is between 800 and 1000 μm/m. Analysis conditions were selected: a capacity of 80 Nm and a safety factor of 2.5 based on the specifications of a typical service robot arm.

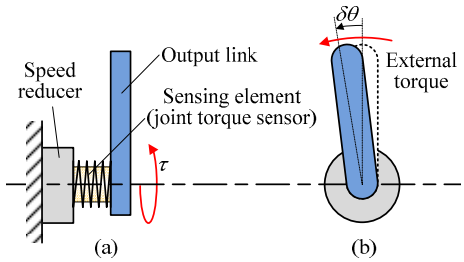

Fig. 1 Deformation of the joint torque sensor: (a) side view, and (b) top view

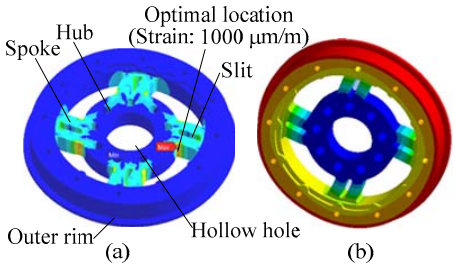

Fig. 2 Analysis for design: (a) FEM analysis, and (b) modal analysis

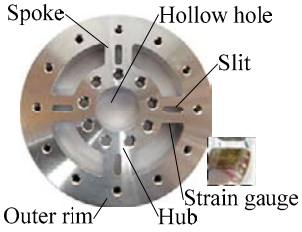

Specifications	
Capacity (Nm)	80
Safety factor	2.5
Size (mm)	ϕ80x12
Weight (g)	102
Rot. stiff. (kNm/°)	2.5
Natural freq. (kHz)	6

Fig. 3 Developed joint torque sensor

Furthermore, a modal analysis shown in Fig. 2(b) was conducted to calculate the natural frequency of the sensor. This natural frequency provides the information on the bandwidth of the sensor, which must be of sufficient range to guarantee high performance in force control and collision detection. Through the FEM analysis and modal analysis, it was found that the rotational stiffness of the structure was 2.5 kNm/°, and the natural frequency was 6 kHz. Based on these results, the joint torque sensor was developed, as shown in Fig. 3. It can be noted that we did not perform any experiments to verify the specifications obtained from the FEM and modal analysis. However, as can be seen from previous studies, there is no need to perform extra experiments as the FEM and modal analysis yields acceptable results.[11]

2.2 Amplifier

Strain gauges are used to measure the deformation of the joint torque sensor. The resistance of a strain gauge changes in proportion to the deformation of the structure that it is attached to, and this resistance change, which is extremely small, is converted to a voltage change by a Wheatstone bridge. A Wheatstone bridge is composed of four strain gauges (SG) attached to the spokes at which maximum strains occur, as shown in Fig. 4(a). Since the full-bridge circuit using four strain gauges sums all the resistance changes of the strain gauges, it amplifies the output by four times.

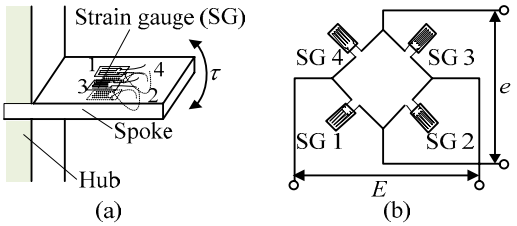

Fig. 4 Wheatstone bridge: (a) installation position of strain gauges, and (b) full-bridge circuit

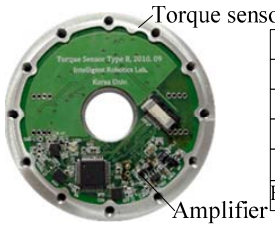

Specifications	
Amplification	400
Channels	2
Processor	CortexM3
Communication	RS-485
Bandwidth (kHz)	1.5

Fig. 5 Amplifier embedded into the joint torque sensor

Also, it compensates for the deformations of the spokes due to a temperature change. The detailed view of the circuit is shown in Fig. 4(b).

The output signal of the Wheatstone bridge is expressed by

$$e = \frac{R_1 R_3 - R_2 R_4}{(R_1 + R_2)(R_3 + R_4)} E \tag{2}$$

where E is the excitation voltage, e is the output signal, and R_1, R_2, R_3 and R_4 are the resistances of the four strain gauges. The voltage level of the output signal e is only a tenth of a mV, and it can be easily contaminated by the noise from other electrical components such as motors. Thus, the output signal should be amplified. The Wheatstone bridge and amplifier must be placed close to each other to prevent the output signal from being contaminated by noise before amplification.

The output signal of a Wheatstone bridge is amplified by a signal amplifier. This amplifier should be placed close to the torque sensor to suppress noise. However, commercial amplifiers are too large to install inside a service robot arm, and thus, an embedded-type torque sensor amplifier was developed in this study. The amplifier has 2 input channels to amplify the output signals from the two Wheatstone bridges. Also, to suppress any electrical noise, an active low-pass filter consisting of resistors, capacitors and operational amplifiers is implemented. An additional software filter (e.g., low-pass filter or band-pass filter) is programmed to further reduce noise. Furthermore, RS-485 communication protocol was implemented to effectively transmit the output signals of multiple torque sensors. This allows a serial connection of all sensors to minimize wiring. The developed amplifier is shown in Fig. 5.

3. Torque ripple reduction

The torque ripple generated by the flexibility of the harmonic drive is a periodical noise which adversely affects the force control and collision detection of a manipulator. Furthermore, its frequency

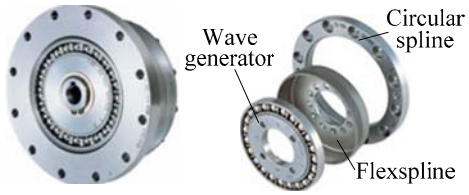

Fig. 6 Components of harmonic drive[12]

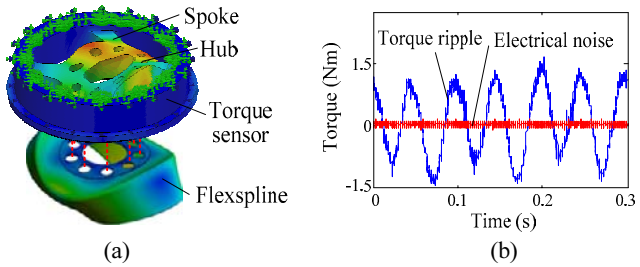

Fig. 7 (a) Effect of deformation of flexspline on joint torque sensor, and (b) torque ripple

depends on the angular velocity of the harmonic drive, so a simple filter is not sufficient to completely remove this torque ripple. In this section, the cause of torque ripple will be analyzed in detail and an effective method of its reduction will be also presented.

3.1 Torque ripple

A harmonic drive is composed of a wave generator, a flexspline and a circular spline as shown in Fig. 6. It is widely used in manipulators due to its light weight, high precision, and high gear reduction.

When a manipulator is operating, the joint torque sensor installed between the flexspline (i.e., the output of the harmonic drive) and the distal link should detect only the torque in its rotational direction to correctly estimate external forces. However, as shown in Fig. 7(a), deformation of the flexspline due to the elliptic shape of the wave generator during the operation of the harmonic drive induces an additional torque, which must be detected by the joint torque sensor. This additional torque induces the deformation of the hub, which lead to twists of the spokes. These twists affect the strain gauges of the Wheatstone bridge. Therefore, each strain gauge is subjected to the two strains, one caused by the applied torque and the other by the twist of the spoke.[7] The output signal of the Wheatstone bridge representing both the torque of interest and the twist of the spoke is given by

$$e = \frac{k \cdot E}{4}(\varepsilon_1 - \varepsilon_2 + \varepsilon_3 - \varepsilon_4 + \varepsilon_t) \tag{3}$$

where k is the gauge factor, ε_1, ε_2, ε_3 and ε_4 are the strains of the four strain gauges and ε_t is the strain due to the twist of the spoke which is the result of the undesirable deformation of the flexspline. Therefore, the output signal of the Wheatstone bridge inevitably includes the torque ripple caused by this deformation.

The output of the torque sensor connected to the flexspline of a harmonic drive was recorded to observe torque ripple. As shown in Fig. 7(b), torque ripple can be expressed as a sinusoidal wave of 3 Nm amplitude (peak-to-peak) when no load is applied and constant

angular velocity is maintained, which is several times higher than amplitude of the electrical noise. Therefore, torque ripple disturbs a torque sensor's ability to accurately measure external torques and consequently, degrades a robot's performance in force control and collision detection. Therefore, torque ripple should be eliminated or suppressed.

The frequency of torque ripple is proportional to the angular velocity ω_w (°/s) of the wave generator because each turn of a wave generator generates two deformation cycles of the flexspline, which correspondingly leads to two periods of torque ripple. In other words, as shown Fig. 8, a half turn of the wave generator generates a period of torque ripple. Therefore, the frequency f (Hz) of torque ripple is expressed by

$$f = \frac{\omega_w}{180} = \frac{r\omega_f}{180} \tag{4}$$

where ω_f (°/s) is the angular velocity of the flexspline, which is the output of the harmonic drive, and r is the speed reduction ratio of the harmonic drive. Also, the value of 180 was used to convert degrees into radians. As described above, torque ripple is periodic, proportional to the rotational velocity of the flexspline. Therefore, it is difficult to eliminate torque ripple when the rotational velocity is changing. In the next section, the proposed method for torque ripple reduction will be discussed in detail.

3.2 Torque ripple reduction

The deformation of the flexspline twists the spokes out of the plane of rotation to some extent, and this twist causes torque ripple. As shown in Fig. 8, since the period of torque ripple is 180°, 90° rotation of the wave generator will generate torque ripple with the opposite phase. Therefore, installing two Wheatstone bridges placed 90° apart, as shown in Fig. 9, will enable simultaneous measurements of two torque ripples of opposite phases.

The two signals are proportional to the external torque, but the torque ripples have opposite phases. The measured signals can be expressed by

$$\begin{aligned} \tau_{B1} &= \tau + A\sin(2\pi ft) \\ \tau_{B2} &= \tau + A\sin(2\pi ft + 2\phi) \end{aligned} \tag{5}$$

where τ_{B1} and τ_{B2} are signals 1 and 2 from bridges 1 and 2, respectively, τ (Nm) is the external torque applied to the joint, A (Nm) is the amplitude of the torque ripple, and f (Hz) is the frequency of the torque ripple, and ϕ (= 90°) is the phase difference between the two signals. As shown in Eq. (5), the two measured signals contain the same external torque and the torque ripples of opposite phases. Taking the average of the two signals yields the external torque of interest as follows:

$$\tau = \frac{(\tau_{B1} + \tau_{B2})}{2} \tag{6}$$

Therefore, torque ripple can be effectively eliminated.

The proposed method does not involve complex computation or the use of a filter. This hardware compensation method does not induce any time delay since no software filtering is involved.

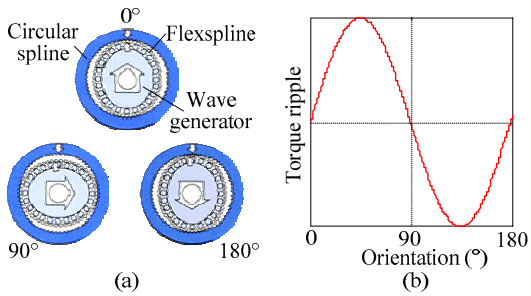

Fig. 8 Relation between orientation of wave generator and period of torque ripple: (a) orientation of wave generator,[12] and (b) torque ripple

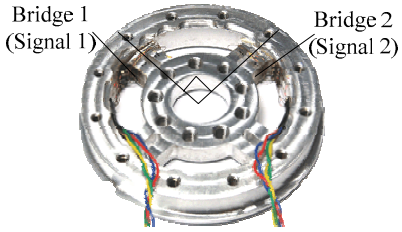

Fig. 9 Two Wheatstone bridges arranged perpendicular to one another

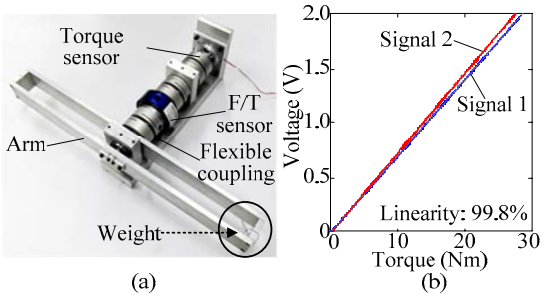

Fig. 10 Static experiments: (a) torque calibrator, and (b) experimental results

4. Experiments and Discussion

The linearity and bandwidth of the proposed joint torque sensor were investigated to verify its performance. In addition, various experiments were conducted to verify the proposed torque ripple reduction method.

4.1 Performance of joint torque sensor

The experimental setup shown in Fig. 10(a) was used for the calibration and performance tests of the developed joint torque sensor. A torque calibrator is composed of a dual arm (for force balance under the initial condition), a commercially available torque sensor as a reference and the developed joint torque sensor. The two torque sensors were connected by couplings to transmit only the rotational torque from the dual arm. Thus, the same torque was applied to the reference torque sensor and the developed joint torque sensor at the same time. In this experiment, two Wheatstone bridge signals were measured as various weights were loaded and unloaded sequentially.

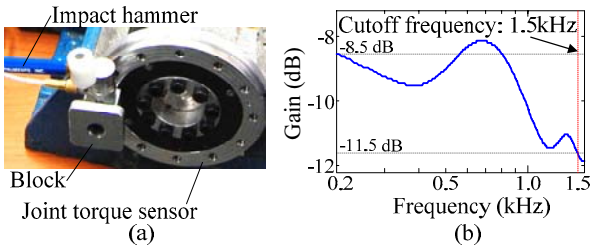

Fig. 11 Dynamic experiments: (a) experimental setup, and (b) experimental results

Figure 10(b) shows the output voltage from each Wheatstone bridge in the joint torque sensor versus the external torque subject to the applied weight at the end of the dual arm. From this result, the torque coefficient, which is the ratio of the torque value to the output voltage, can be computed using the least-squares method. Moreover, the high linearity of 99.8% for both Wheatstone bridges guaranteed the precision of the torque measurements.

A joint torque sensor of a multi-DOF service robot arm should have enough bandwidth to achieve high performance in force control and collision detection. The experimental setup shown in Fig. 11(a) was constructed to evaluate the response time of the developed sensor including its amplifier. An impact was generated using an impact hammer as it hit a block mounted at the outer rim of the joint torque sensor while the hub of the torque sensor was fixed. The recorded data were processed using a dual channel FFT analyzer and the resulting bode plot is shown in Fig. 11(b). As shown in Fig. 11(b), the gain decreased by 3 dB (from -8.5 dB to -11.5 dB) at the frequency of 1.5 kHz, which corresponds to the cutoff frequency of the amplifier of the joint torque sensor.

4.2 Torque ripple reduction

The experimental setup shown in Fig. 12 was constructed to evaluate the proposed method for torque ripple reduction. The joint module consists of a harmonic drive, a joint torque sensor, a cross-roller bearing and a hollow shaft. A component-type harmonic drive, which has a reduction ratio of 160, maximum average load torque of 75 Nm and a mass of 240 g, was used for this experiment. The capacity of the harmonic drive is similar to that of the developed joint torque sensor. The joint torque sensor with two Wheatstone bridges was directly connected to the harmonic drive. A cross-roller bearing was used to support the moment load applied to the joint torque sensor (i.e., the moments in directions other than the direction of interest) so that only the rotational torque could be applied to the joint torque sensor. The constructed robot arm was operated through a motor and a belt-pulley connection, and thus, the motor torque was transmitted to the link via the joint module including the proposed joint torque sensor. To verify the torque ripple reduction method, various experiments were conducted at both constant and variable angular velocities.

First, a torque signal was recorded when the robot arm was rotated from 0° to 30° at a constant angular velocity of 20°/s, and the results are presented in Fig. 13(a). Torque signals 1 and 2 were measured from the Wheatstone bridges, respectively, installed at the joint torque sensor as shown in Fig. 9, and the average torque signal

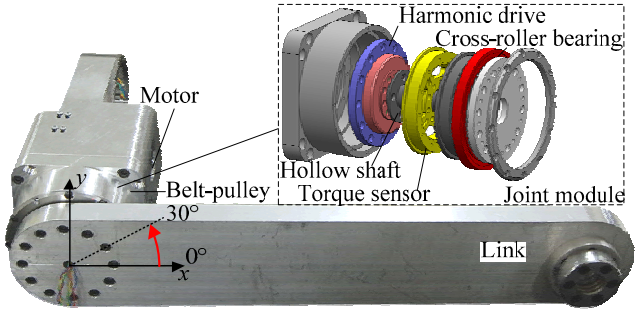

Fig. 12 Experimental setup for torque ripple reduction

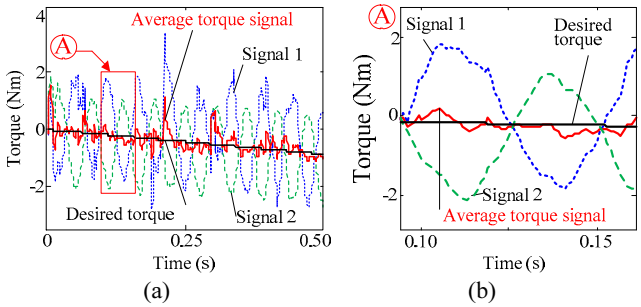

Fig. 13 Experimental results of constant angular velocity of robot joint: (a) general view, and (b) expanded view

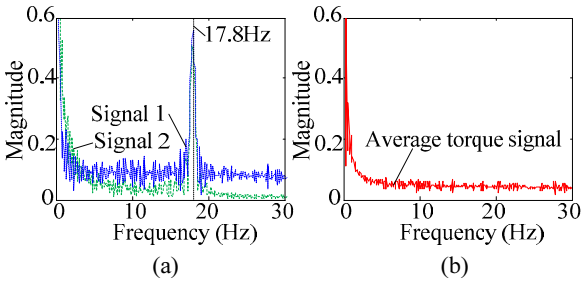

Fig. 14 FFT plots: (a) before torque ripple reduction, and (b) after torque ripple reduction

was also plotted. As shown in Fig. 13(b), the amplitude of the torque ripple was clearly reduced.

Furthermore, the frequency of the torque ripple was calculated as 17.8 Hz using Eq. (4) where a reduction ratio of the harmonic drive was 160 and the angular velocity of the robot joint was 20 °/s. Figure 14(a) shows the FFT plot of both torque signals; there is a large peak at 17.8 Hz, which corresponds to the torque ripple. Figure 14(b) shows the FFT plot of the average torque signal, with no peak at 17.8 Hz. This verifies that the proposed method successfully removed the torque ripple.

Second, torque signals were also measured when the robot arm rotated from 0° to 90°. A 5th-order polynomial was used for the angular velocity profile changing continuously from 0 °/s to 40 °/s as shown in Fig. 15. Figure 16(a) shows the desired torque signal calculated from the link model and the measured torque signals, and Fig. 16(b) shows the desired and filtered torque signals. The amplitude of the torque ripple was clearly reduced but the frequency of the torque ripples was constantly changing.

It should be noted that once the torque ripple is removed using the proposed method, the filtered torque signal shows good

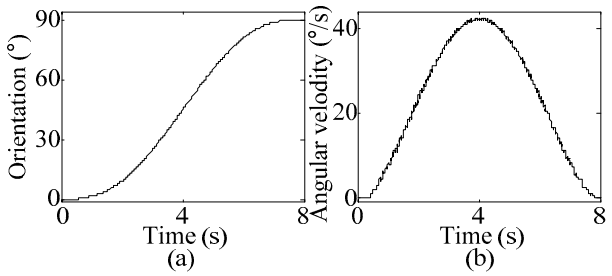

Fig. 15 Motion of link: (a) orientation, and (b) angular velocity

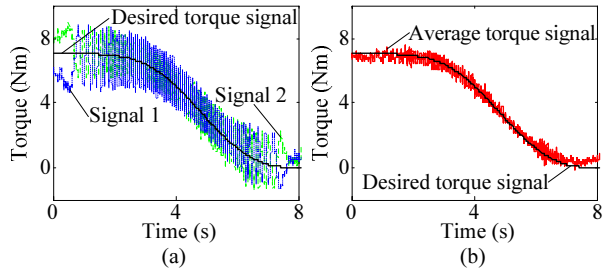

Fig. 16 Experimental results: (a) torque signals, and (b) average torque signal after torque ripple reduction

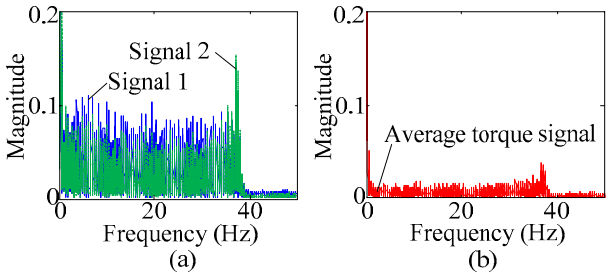

Fig. 17 FFT plots: (a) before torque ripple reduction, and (b) after torque ripple reduction

agreement with the desired torque. This implies that the proposed torque sensor can accurately measure a joint torque.

As the angular velocity of the link changes within 0 °/s to 40 °/s, the frequencies of torque ripple also varies from 0 Hz to 40 Hz as can be seen using Eq. (4). Figure 17(a) and (b) show the FFT plot of the torque signals and the average torque signal, respectively. The FFT plot of the average torque signal shows that the torque ripple was clearly reduced even when the angular velocity, i.e. the frequency of the ripple, constantly changed. Therefore, a torque ripple can be effectively reduced by taking the average of the torque signals from the two Wheatstone bridges, installed perpendicular to one another, without the need for any additional complex software filter algorithms, which would inevitably induce a time delay.

5. Conclusions

This paper proposed a compact joint torque sensor embedded with an amplifier for a service robot arm to minimize noise and wiring. Furthermore, a torque ripple reduction method using two Wheatstone bridges was proposed. Based on our analysis and experimental results, the following conclusions are drawn.

1. The developed joint torque sensor, compact in size, could be easily installed at each joint of a service robot. The amplifier was embedded into the sensor module, so no additional circuitry or hardware was needed.
2. Torque ripple was greatly reduced by taking the average of the torque signals from the two Wheatstone bridges installed perpendicular to one another. This method did not require the use of a filter to prevent any time delay.

ACKNOWLEDGEMENT

This work was supported by Human Resources Development Program for Convergence Robot Specialists (MKE) (NIPA-2012-H1502-12-1002) and by the National Research Foundation of Korea funded by the Ministry of Education, Science and Technology (No. 2012-0000792).

REFERENCES

1. Gravel, D. P. and Newman, W. S., “Flexible robotic assembly efforts at Ford Motor Company,” Proc. of the IEEE International Symposium on Intelligent Control, pp. 173-182, 2001.
2. Tsetserukou, D., Tadakuma, R., Kajimoto, H., Kawakami, N., and Tachi, S., “Development of a Whole-Sensitive Teleoperated Robot Arm using Torque Sensing Technique,” Proc. of the IEEE International Conference on Intelligent Robots and Systems, pp. 476-481, 2007.
3. Hirzinger, G., Sporer, N., Albu-Schaffer, A., Hahnle, M., Krenn, R., Pascucci, A., and Schedl, M., “DLR's torque-controlled light weight robot III-are we reaching the technological limits now?” Proc. of the IEEE International Conference on Robotics and Automation, pp. 1710-1716, 2002.
4. DLR, “Institute of Robotics and Mechatronics, Status Report 1997-2004,” Part 1, pp. 35-42, 2004.
5. Tuttle, T. D. and Seering, W. P., “A nonlinear model of a harmonic drive gear transmission,” IEEE Int. Conf. on Robotics and Automation, Vol. 12, No. 3, pp. 368-374, 1996.
6. Dhaouadi, R., Ghorbel, F. H., and Gandhi, P. S., “A new dynamic model of hysteresis in harmonic drives,” IEEE Trans. on Industrial Electronics, Vol. 50, No. 6, pp. 1165-1171, 2003.
7. Taghirad, H. D. and Belanger, P. R., “Torque ripple and misalignment torque compensation for the built-in torque sensor of harmonic drive systems,” IEEE Trans. on Instrumentation and Measurement, Vol. 47, No. 1, pp. 309-315, 1998.
8. Godler, I., Ninomiya, T., and Horiuchi, M., “Ripple compensation for torque sensors built into harmonic drives,” IEEE Trans. on Instrumentation and Measurement, Vol. 50, No. 1, pp. 117-122, 2001.
9. Sensinger, J. W. and Weir, R. F., “Improved torque fidelity in

harmonic drive sensors through the union of two existing strategies," IEEE/ASME Trans. on Mechatronics, Vol. 11, No. 4, pp. 457-461, 2006.

10. Kim, J. H., Kim, Y. L., and Song, J. B., "A Switching Notch Filter for Reducing the Torque Ripple Caused by a Harmonic Drive in a Joint Torque Sensor," Trans. of the KSME (A), Vol. 35, No. 7, pp. 709-715, 2011.
11. Aghili, F., Buehler, M., and Hollerbach, J. M., "Design of a Hollow Hexaform Torque Sensor for Robot Joints," The International Journal of Robotics Research, Vol. 20, No. 12, pp. 967-976, 2001.
12. Samick HDS Co. LTD., http://www.shds.co.kr